

**Bericht des Instituts für Aerodynamik und Strömungstechnik
Report of the Institute of Aerodynamics and Flow Technology**

IB 124-2010/3

**Evaluation of the BLWF Code –
A Tool for the Aerodynamic Analysis of Transonic
Transport Aircraft Configurations**

Ke-shi Zhang, Martin Hepperle

Herausgeber:

Deutsches Zentrum für Luft- und Raumfahrt e.V.
in der Helmholtz Gemeinschaft
Institute of Aerodynamics and Flow Technology
Lilienthalplatz 7, D-38108 Braunschweig

ISSN 1614-7790

Access Level: 1
Braunschweig, July 2010

Head of Institute:
Prof. Dr.-Ing. habil. C.-C. Rossow

Authors:
Dr. K.S. Zhang
Dr. M. Hepperle

Branch: Configuration Design
Head of Branch:
Prof. Dr.-Ing. H. Geyr von Schweppenburg

This Report contains:
25 pages
20 figures
3 references



Abstract

The BLWF code [1] was developed by researchers at the Central Aerohydrodynamic Institute (TsAGI). The BLWF code has been developed for preliminary aerodynamic analysis of transonic transport aircraft configurations. It can be used for rapid computations of viscous transonic flow over wing/body/nacelle/ tail configurations.

Numerical simulations of the flow past the DLR-F6 wing-body configuration have been performed to evaluate the accuracy and efficiency of this code, when used for preliminary aerodynamic analysis of transonic transport configurations.

A brief description of computational methods is given in Section 1. The numerical results and discussion are given in Section 2. The computational results for a prescribed Mach number ($Ma=0.75$) and prescribed design lift coefficient ($C_L=0.5$) are compared with the available experimental data. The effect of Mach number on the aerodynamic performance is investigated by computations at Mach numbers from 0.2 to 0.9, with fixed Reynolds number and varying angles of attack.

According to the evaluation results, the BLWF code is well suited for the preliminary aerodynamic analysis of transonic transport aircraft configurations.



1 Table of Contents

Abstract.....	3
1 Table of Contents.....	4
2 Computational Methods.....	5
2.1 Computational method of BLWF code	5
2.2 Computation of total drag incl. form drag of fuselage	5
3 Numerical results.....	6
3.1 Validation of code for prescribed Mach number ($Ma=0.75$).....	6
3.2 Validation of code for prescribed lift coefficient ($C_L=0.5$).....	7
3.3 Effect of Mach number on aerodynamic performance.....	7
4 Conclusions.....	8
References.....	9
Figures.....	10

2 Computational Methods

2.1 Computational method of BLWF code

The computational method of BLWF code is briefly stated as following:

- External inviscid flow:
Solution of the conservative full potential equation;
"Chimera" technique for complex configurations
- Viscous boundary layer region:
Finite-difference inverse method for calculation of 3-D compressible laminar and turbulent boundary layers;
2-d integral or 3-d finite-difference method for viscous wake calculations
- Viscous-inviscid coupling:
Quasi-simultaneous viscous-inviscid coupling scheme

A detailed description of the methods implemented in the BLWF code can be found in reference [1].

2.2 Computation of total drag incl. form drag of fuselage

The current version of BLWF code (BLWF56) does not calculate the form drag of the fuselage (only the induced drag, wave drag and profile drag of wing are considered). Therefore this report uses an empirical formula to calculate the form drag of the fuselage. It takes the form of

$$C_{D\text{Body}} = C_f * S_{\text{wet}} / S_{\text{ref}} * F_{\text{form}} \quad (1)$$

where F_{form} is the form factor (F_{form} for a clean airliner fuselage is about 1.1), $S_{\text{wet}}/S_{\text{ref}}$ represents the ratio of wetted surface area and reference area ($S_{\text{wet}}/S_{\text{ref}}$ for the DLR-F6 model is 2.93), and C_f is the skin friction coefficient of a turbulent flat plane. The following formula² is used for calculating C_f .

$$C_f = \frac{0.455}{(\log_{10} Re)^{2.58} (1 + 0.144 Ma^2)^{0.65}} \quad (2)$$

where Re is the fuselage Reynolds number based on the length of fuselage.

After the form drag of fuselage is obtained, the total drag coefficient for the wing/body configuration can be calculated by

$$C_D = C_{D\text{IND}} + C_{D\text{WAVE}} + C_{D\text{FP}} + C_{D\text{Body}} \quad (3)$$

where $C_{D\text{IND}}$, $C_{D\text{WAVE}}$ and $C_{D\text{FP}}$ are the induced, wave and profile drag coefficients given by BLWF code. Note that it is important to consider the form drag of the fuselage to achieve a consistent comparison with the experimental data.

3 Numerical results

The simulation of the flow past the DLR-F6 wing-body configuration is taken as a test case for the evaluation of BLWF code. A comparison with wind tunnel test data is presented. The wind tunnel model and the surface grid for CFD computation are shown in Fig. 1 and Fig. 2.

The following are some parameters of the wind tunnel model reference geometry:

- Moment reference point (from fuselage nose): 504.9 mm
 - Projected half span (v-form 4.787 deg): 585.647 mm
 - Half model reference area: 72700.0 mm²
 - Mean aerodynamic chord: 141.2 mm
 - Fuselage length: 1192 mm
 - Reynolds number based on the average aerodynamic chord of wing: 3×10^6 .
- The most important details of the wind tunnel model DLR-F6 can be found on the web site [3].

3.1 Validation of code for prescribed Mach number (Ma=0.75)

The computations at different angles of attack with a prescribed Mach number (Ma=0.75) are performed and the accuracy of the code is evaluated by comparison with the experimental data, shown in Fig. 3~Fig. 9. Fig. 3 illustrates the lift-to-drag ratio versus lift coefficient. It can be concluded that near the design lift coefficient, 0.5, the predicted maximum L/D is a little bit higher than the experimental value. It might be caused by the under-prediction of drag and over-prediction of lift. The predicted maximum L/D is about 18 and 5.9% higher than the experimental value. Fig. 4 shows the lift-to-drag ratio versus angle of attack. Similar to that shown in Fig. 3, the predicted value is higher than the experimental value. Fig. 5 gives the drag polar curve, which indicates that the minimum drag is under predicted by about 20%. Fig. 6 illustrates the lift coefficient versus angle of attack. It seems like that the difference between the predicted value and the experimental data is a constant. That is possibly caused by the computational scheme or the wind tunnel side effect. Fig. 7 shows the total drag coefficient versus angle of attack, which indicates that the drag is under predicted at lower angle of attack and over predicted at higher angle of attack. It might be caused by the facts that by using such a code the viscous drag at lower angle of attack can be under predicted and the shock wave drag at higher angle of attack can be over predicted. Fig. 8 shows the pitching moment coefficient versus lift coefficient and Fig. 9 shows the pitching moment coefficient versus angle of attack. It shows that the absolute value of predicted C_M is larger than the experimental data. The reason may be due to the fact that the location of shock wave computed by full-potential equation is behind the one from experimental data.

Each computation costs about 35 seconds on a Pentium (R) 4 CPU personal computer of 2.80 GHz. As the computation can be highly efficiently performed with reasonable accuracy, it can be concluded that this code is well suitable for preliminary aerodynamic design.

3.2 Validation of code for prescribed lift coefficient ($C_L=0.5$)

The computations at different Mach numbers with a prescribed lift coefficient ($C_L=0.5$) are performed and the accuracy of the code is evaluated by comparison with experimental data. Fig. 10~Fig. 12 illustrate how Mach number affects the total drag coefficient, lift-to-drag ratio and pitching moment. In Fig. 10 the predicted drag is in reasonably good agreement with the experimental data at Mach numbers from 0.6 to 0.8. The predicted value is about 7% lower than the experimental data. Fig. 11 shows that the predicted L/D is about 5.5% higher than the experimental data. In Fig. 12 it is shown that the absolute value of pitching moment is over predicted, which is possibly due to the fact that the location of shock wave computed by full-potential equation is behind the one from experimental data.

Each computation costs about 1 minute and 40 seconds on a Pentium (R) 4 CPU personal computer of 2.80 GHz. The computations with prescribed lift coefficient are efficiently performed with reasonable accuracy, which make it promising to be used for the preliminary aerodynamic design.

3.3 Effect of Mach number on aerodynamic performance

The aerodynamic performance of DLR-F6 is analyzed at different Mach numbers using BLWF code, which shows the effect of Mach number. The results are shown in Fig. 13~Fig. 19. Fig. 13 illustrates the lift-to-drag ratio versus lift coefficient. The results at Mach numbers from 0.2 to 0.7 and from 0.8 to 0.9 are shown in Fig. 13-(a) and Fig. 13-(b), respectively. The results of the lift-to-drag ratio v.s. angle of attack, the drag polar curves, the lift coefficient v.s. angle of attack, the total drag v.s. angle of attack, the pitching moment coefficient v.s. angle of attack and lift coefficient are illustrated in figures from Fig. 14 to Fig. 19, respectively. These figures indicate that at lower Mach number the curves are close to each other and at higher Mach number the difference between curves become apparent due to the shock wave. The effect of Mach number on the zero lift drag coefficient is shown in Fig. 20. The drag divergence Mach number can be calculated from this figure. According to the Boeing definition of divergence drag, $\partial C_{D0}/\partial \alpha > 0.1$, the drag divergence Mach number, Ma_{dd} , is 0.82. Note that near the drag divergence Mach number, the curve is not so smooth due to the failure of computation for some points.

As the compressibility effect is reasonably well predicted by this code, it can be concluded that BLWF code is well suitable for subsonic and transonic aerodynamic analyses, and an major improvement when compared with incompressible panel codes.

4 Conclusions

The BLWF code has been evaluated by the simulation of flow past the DLR-F6 wing-body configuration. The accuracy has been evaluated by comparison of experimental data and the computational results at different angles of attack with a prescribed Mach number ($Ma=0.75$) and at different Mach numbers with a prescribed lift coefficient ($C_L=0.5$). The aerodynamic performance of DLR-F6 wing/body configuration was also analyzed at different Mach numbers to study the effect of Mach number and evaluate this code with respect to compressibility effects.

In general the BLWF code proved to be well suited for the preliminary aerodynamic analysis of transonic transport aircraft configurations. Although the lift and pitching moment are somewhat over-predicted and the drag coefficient is under-predicted, the accuracy is acceptable for preliminary aircraft design. The compressibility and viscous effects can be appropriately considered compared with the common-used panel codes.

In terms of performance the code is faster than Euler or Navier-Stokes solvers by several orders of magnitude. This speed makes the code especially useful for application in preliminary aircraft design.

References

- [1] Karas, O.V., Kovalev, V.E. BLWF 56 User's Guide, 2005.
- [2] Raymer, D.P. Aircraft Design: A Conceptual Approach (Third Edition). American Institute of Aeronautics and Astronautics, Inc., Reston, Virginia, 1999.
- [3] DLR-F6 model details at "[http:// aaac.larc.nasa.gov/tsab/cfdlarc/aiaa-dpw/Workshop2/](http://aaac.larc.nasa.gov/tsab/cfdlarc/aiaa-dpw/Workshop2/)".

Figures



Fig. 1 DLR-F6 with VHBR nacelles in ONERA S2MA wind tunnel.

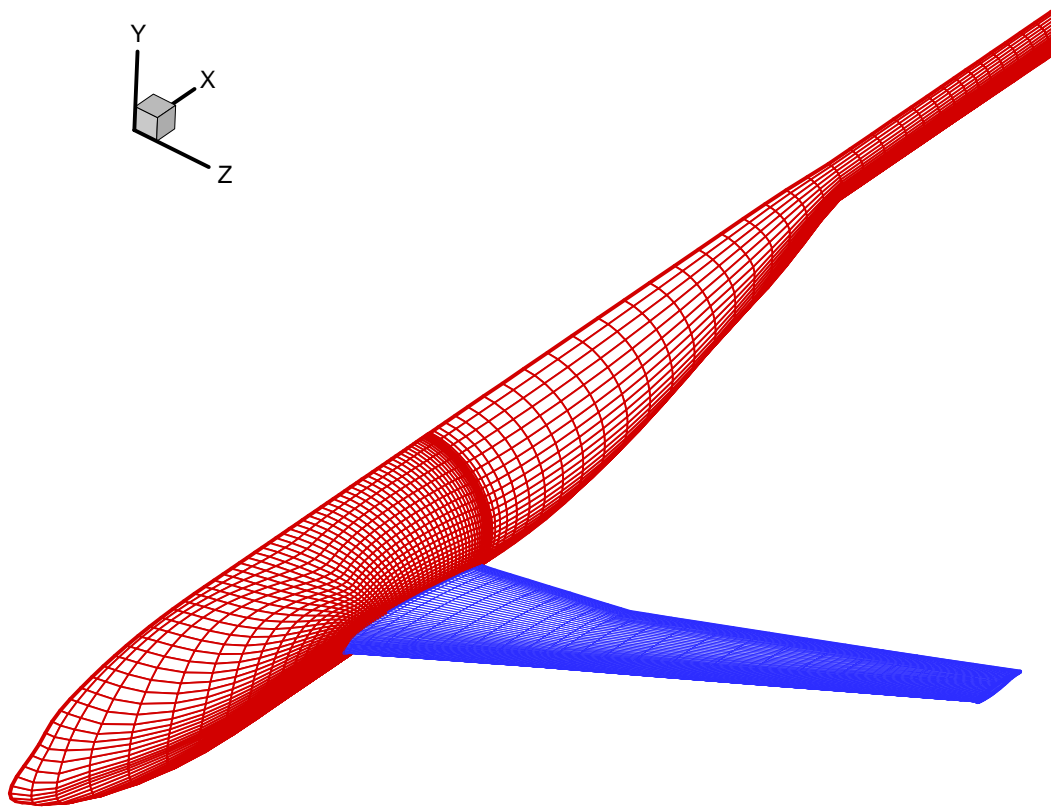


Fig. 2 Surface grid for the DLR-F6 wing-body configuration.

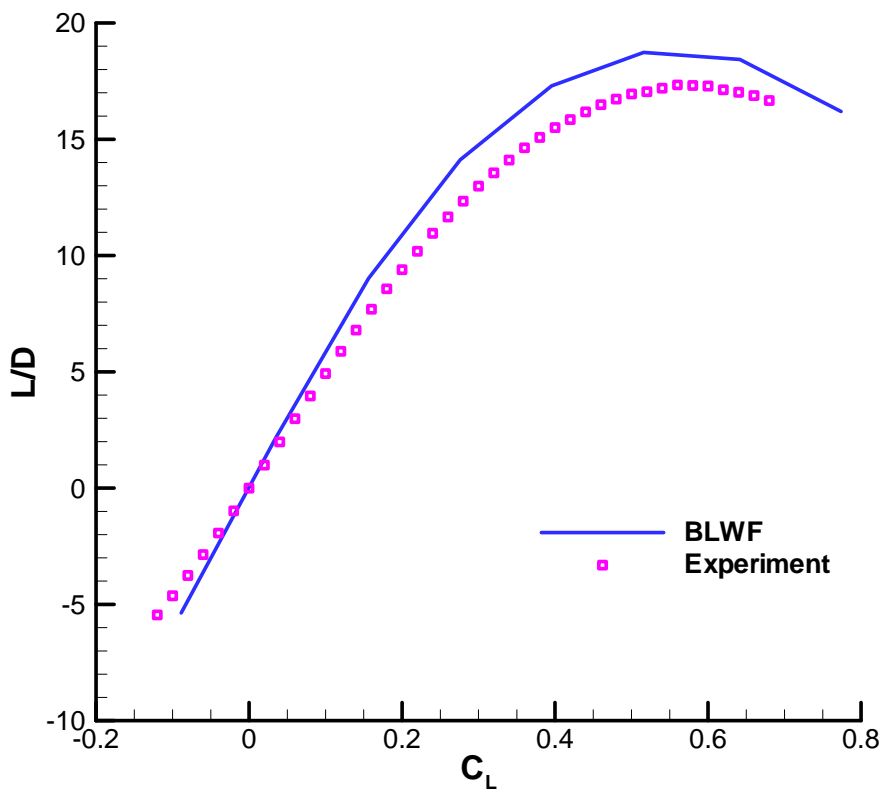


Fig. 3 Lift-to-drag ratio v.s. lift coefficient.

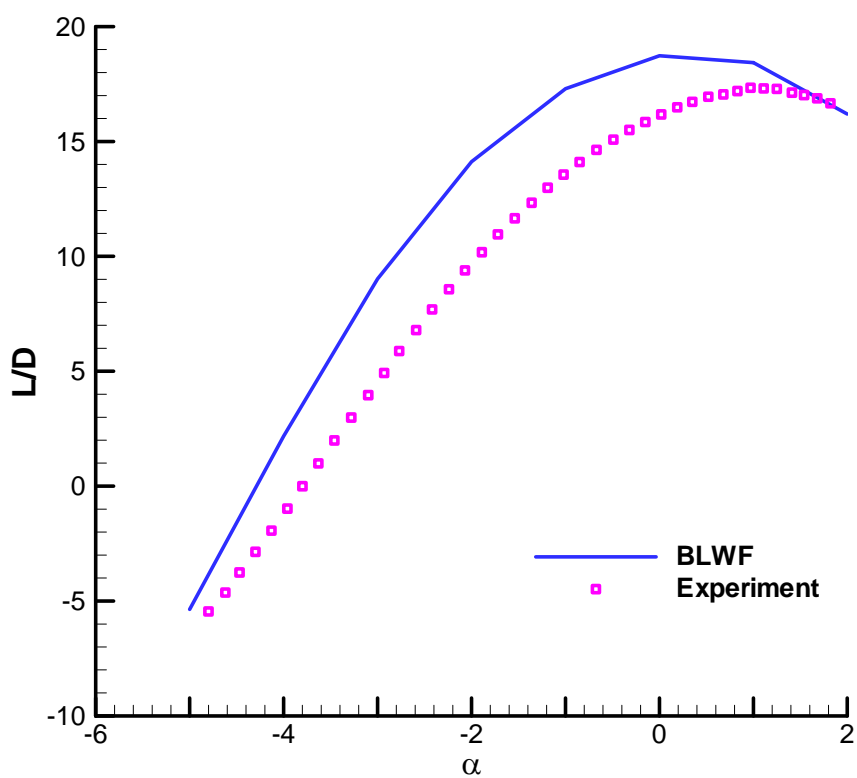


Fig. 4 Lift-to-drag ratio v.s. angle of attack.

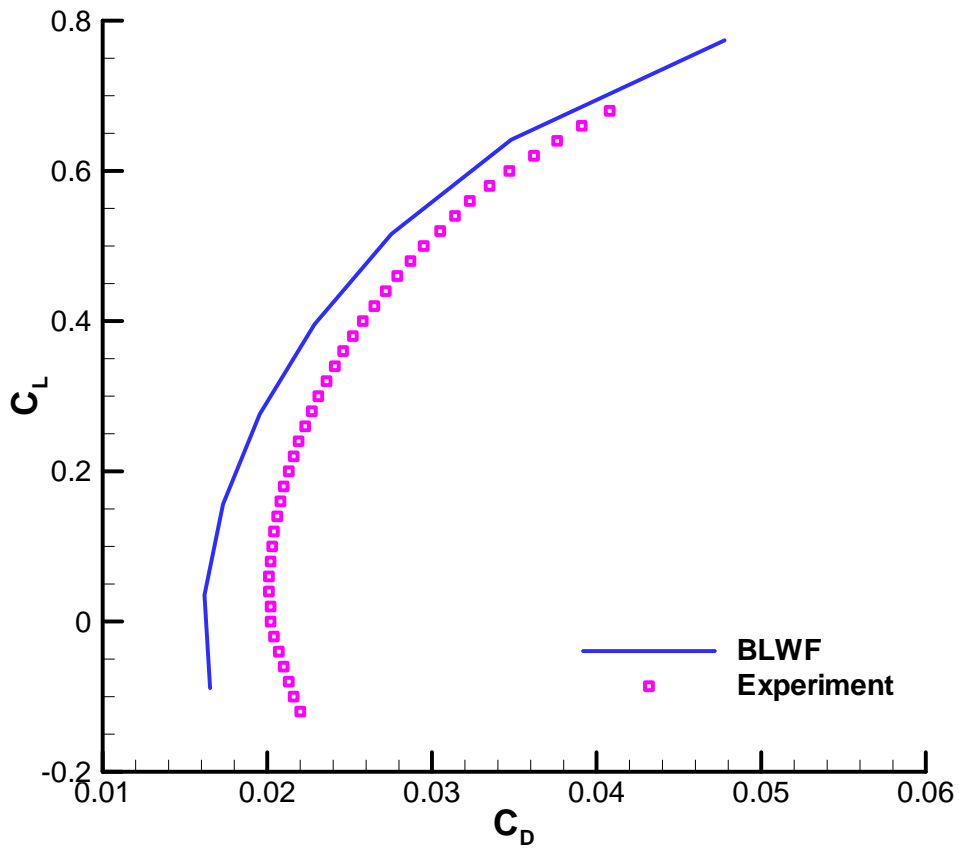


Fig. 5 Lift coefficient v.s. drag coefficient.

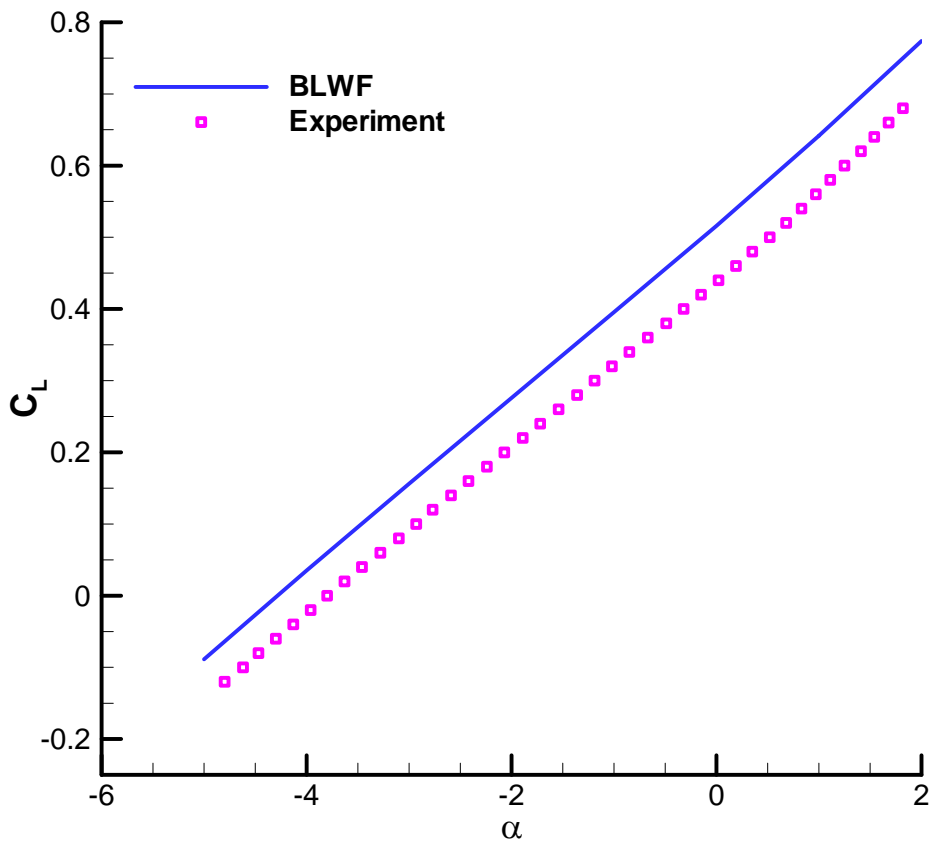


Fig. 6 Lift coefficient v.s. angle of attack.

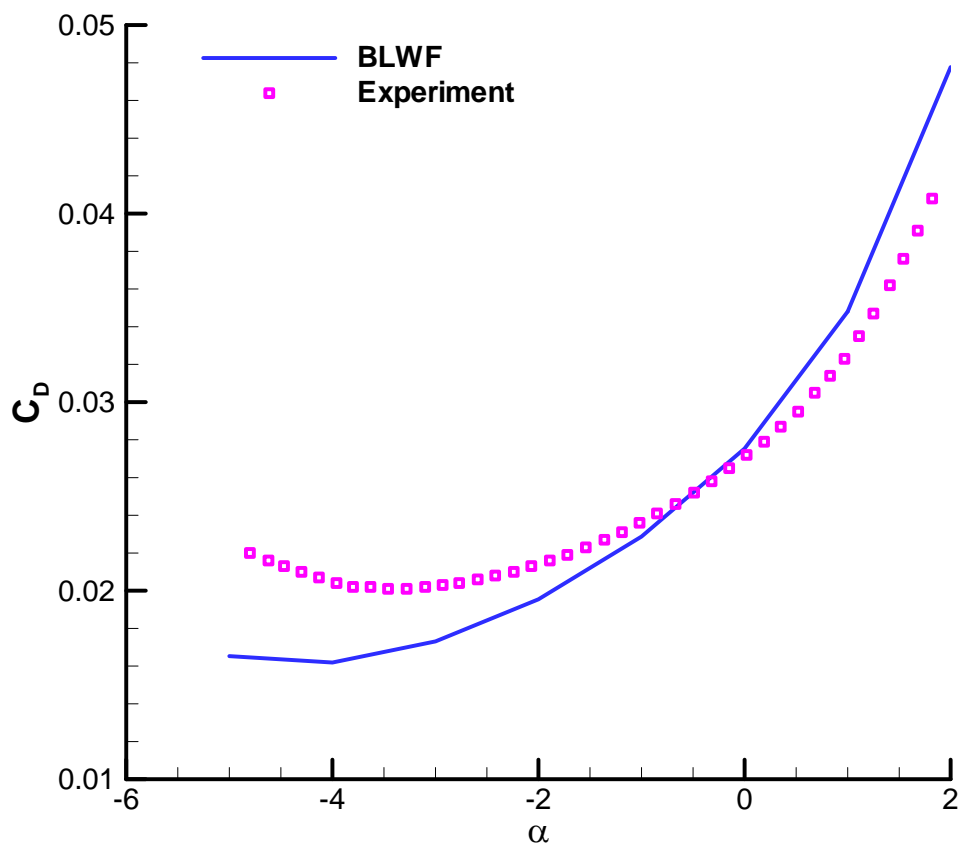


Fig. 7 Total drag coefficient v.s. angle of attack.

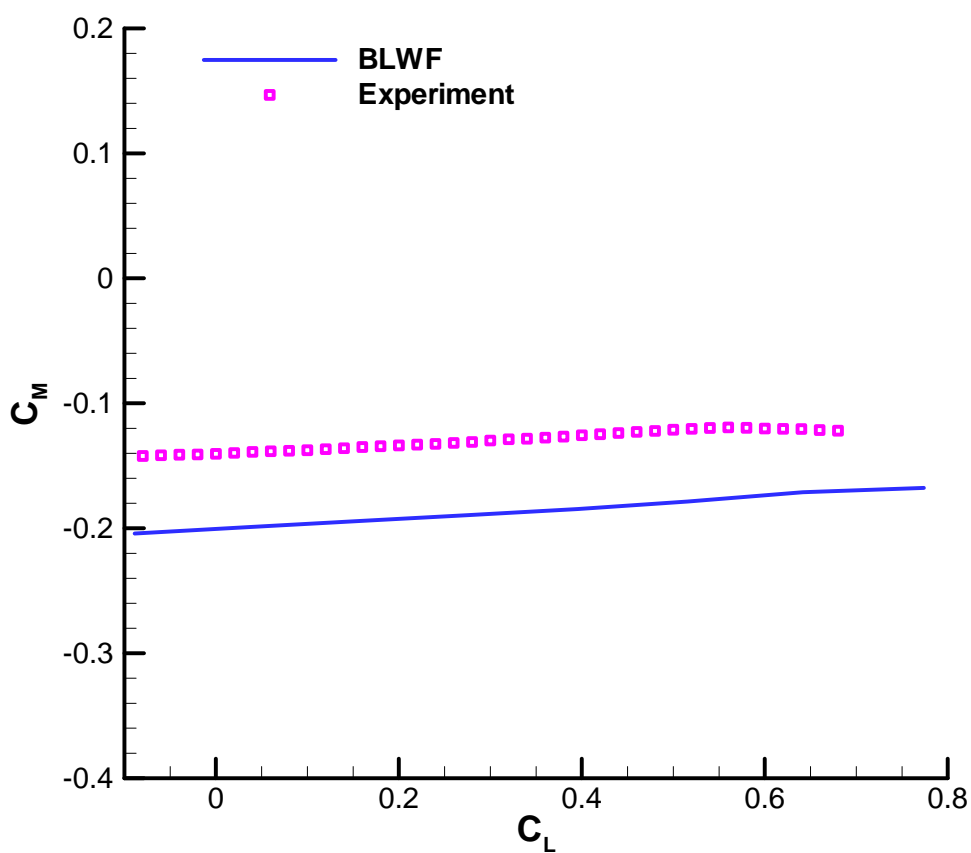


Fig. 8 Pitching moment coefficient v.s. lift coefficient.

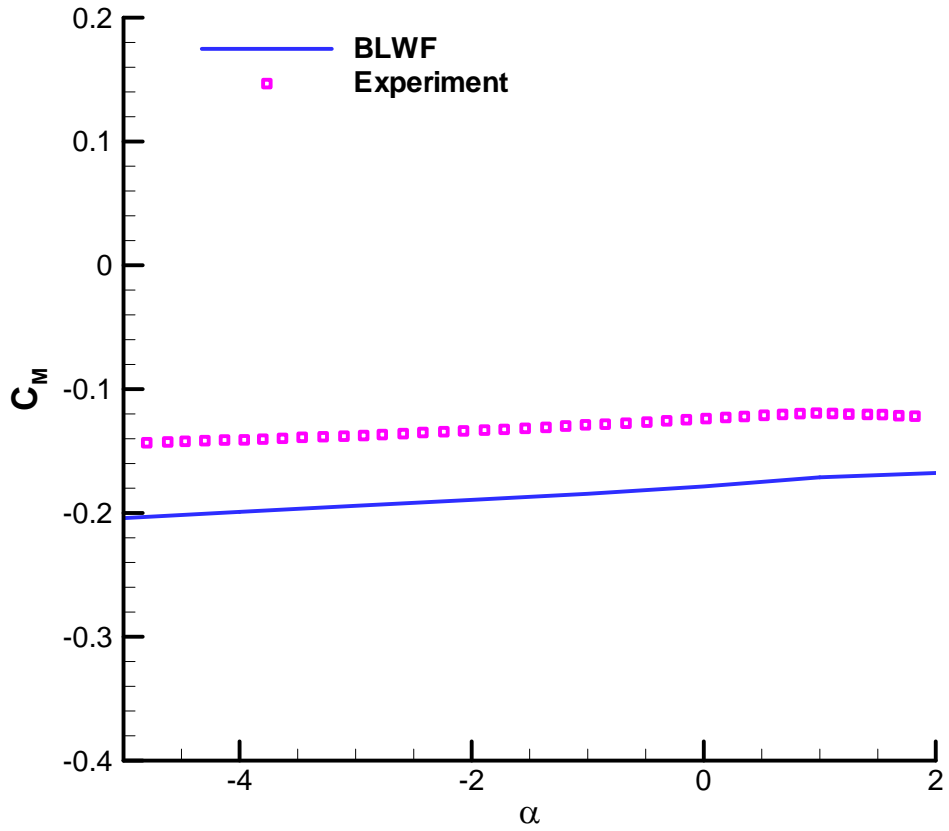


Fig. 9 Pitching moment coefficient v.s. angle of attack.

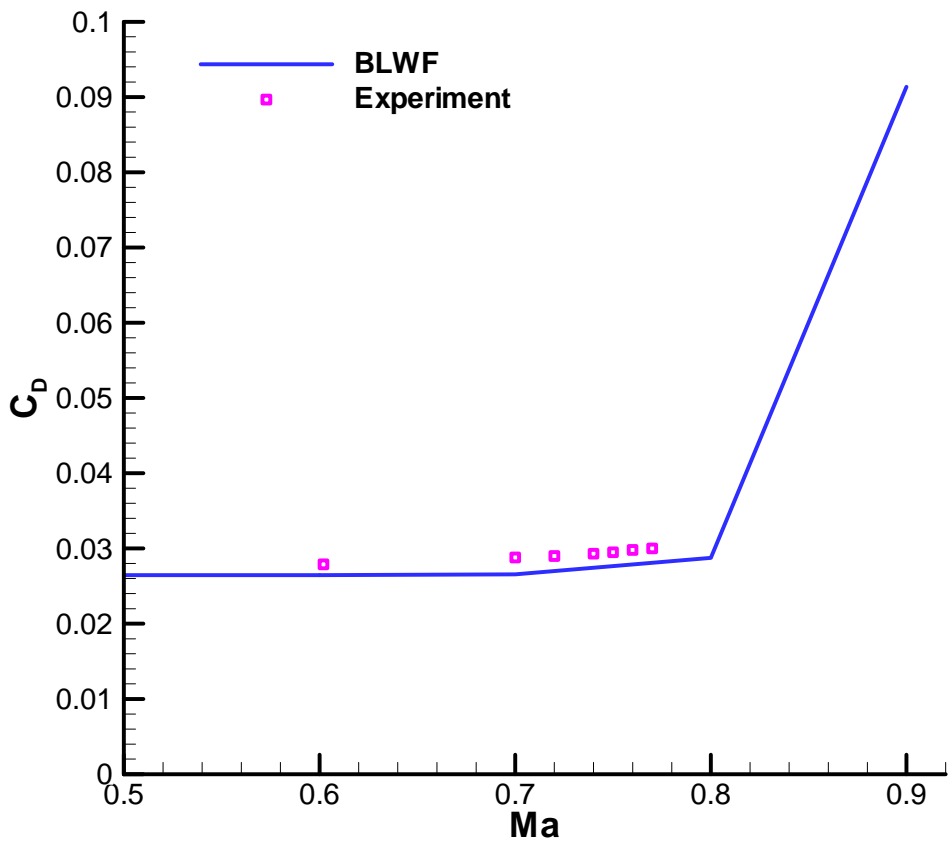


Fig. 10 Total drag coefficient v.s. Mach number.

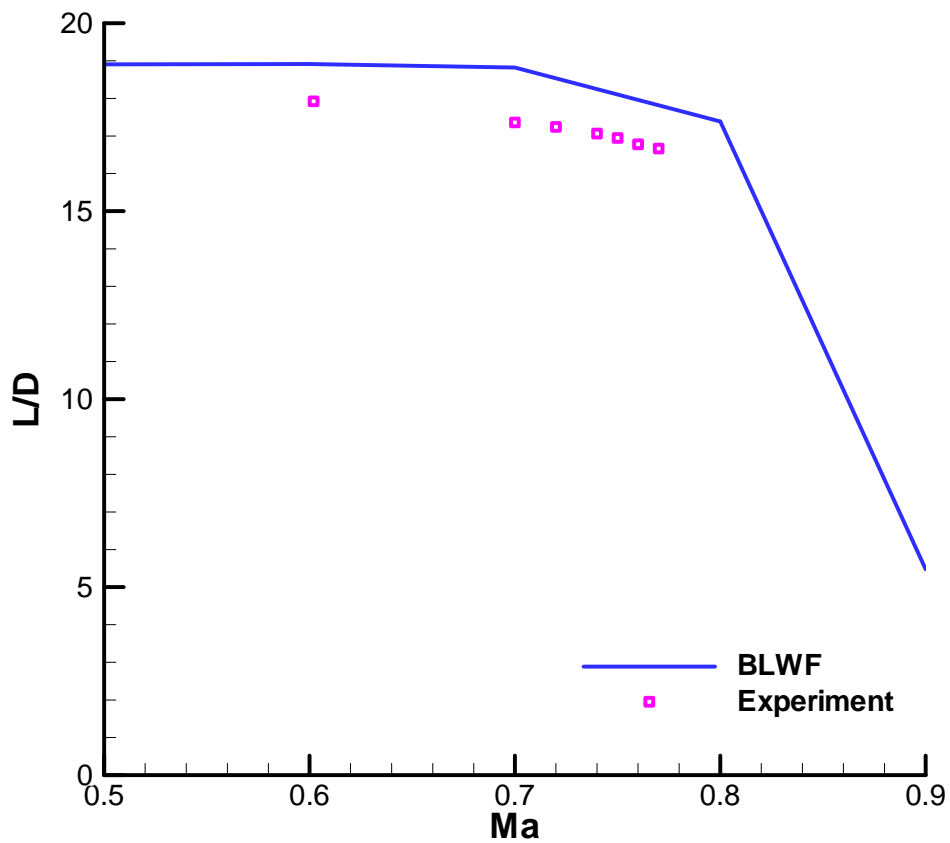


Fig. 11 Lift-to-drag ratio v.s. Mach number.

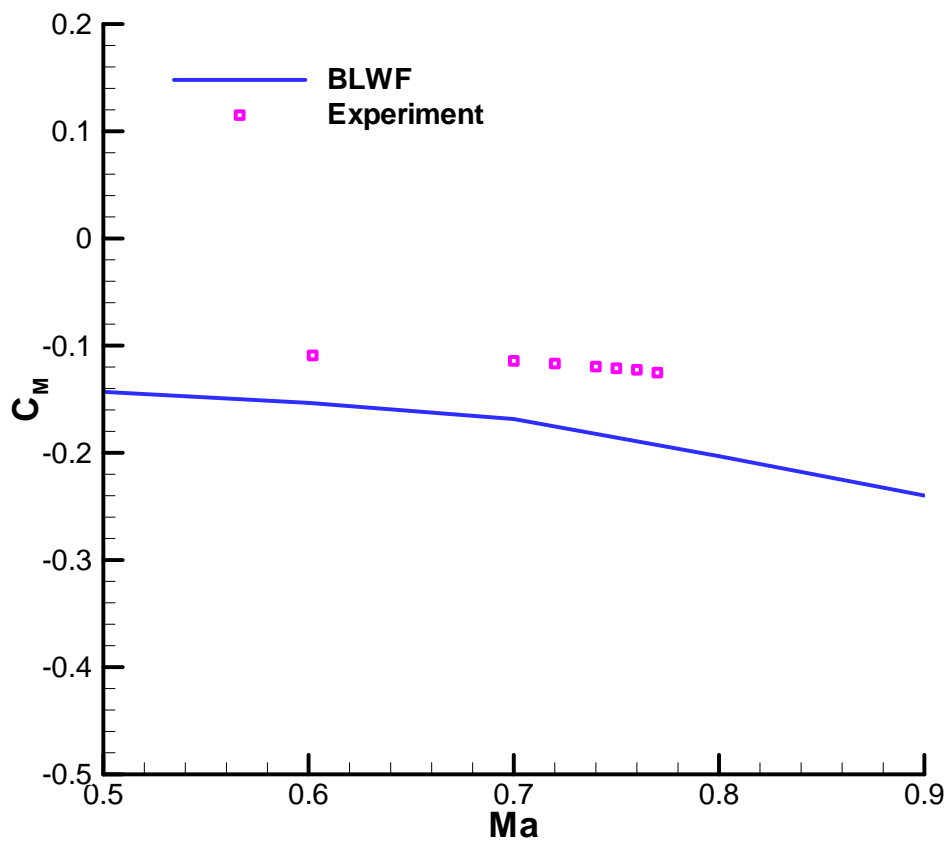
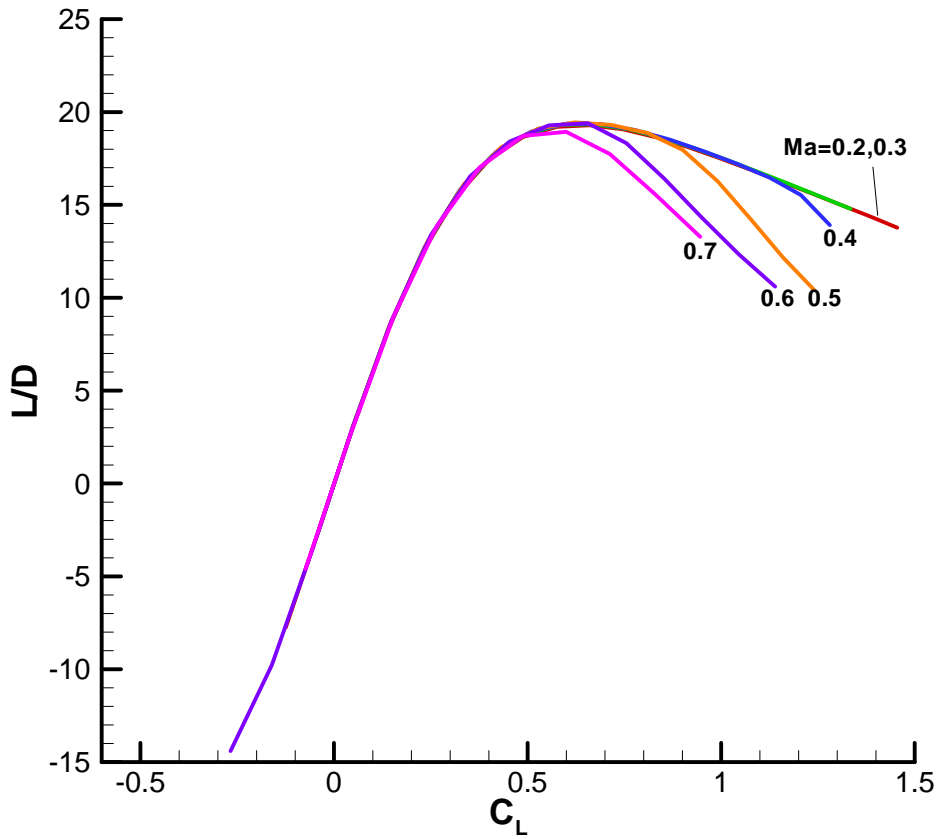
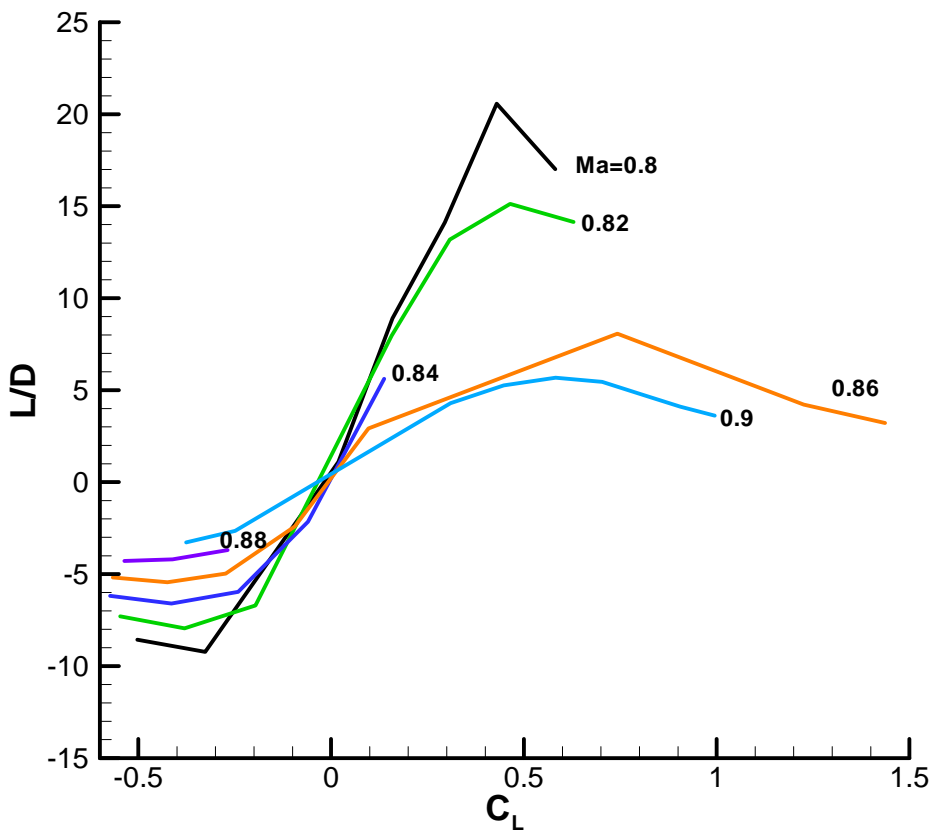


Fig. 12 Pitching moment coefficient v.s. Mach number.

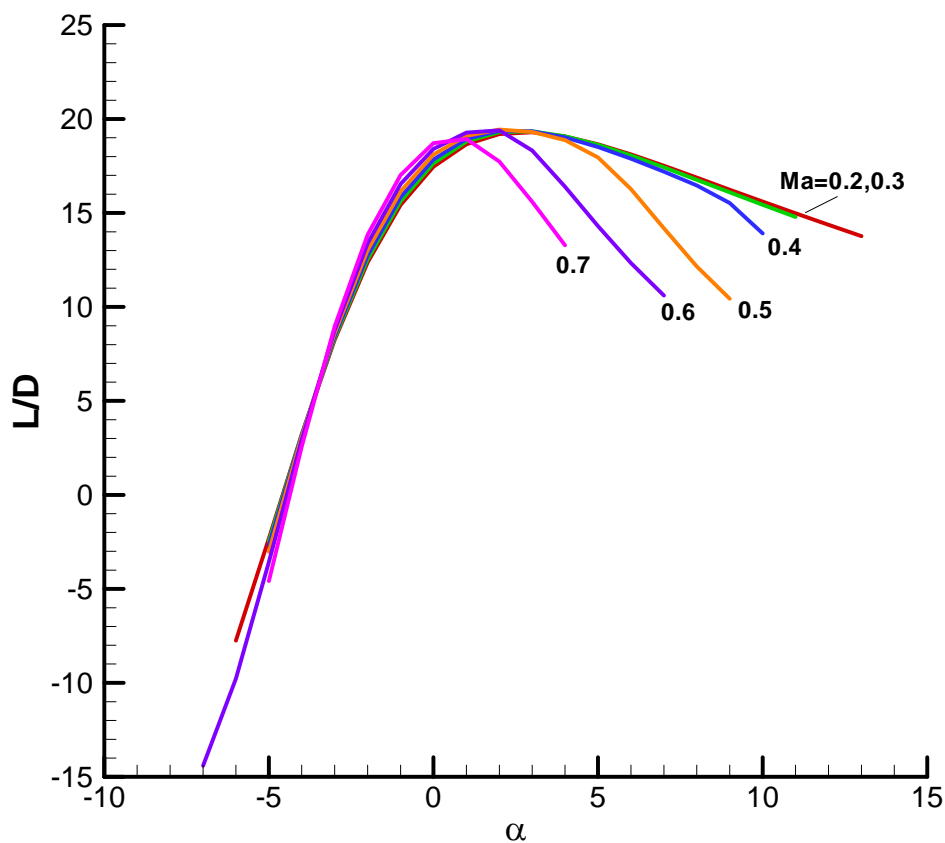


(a) $Ma=0.2 \sim 0.7$.

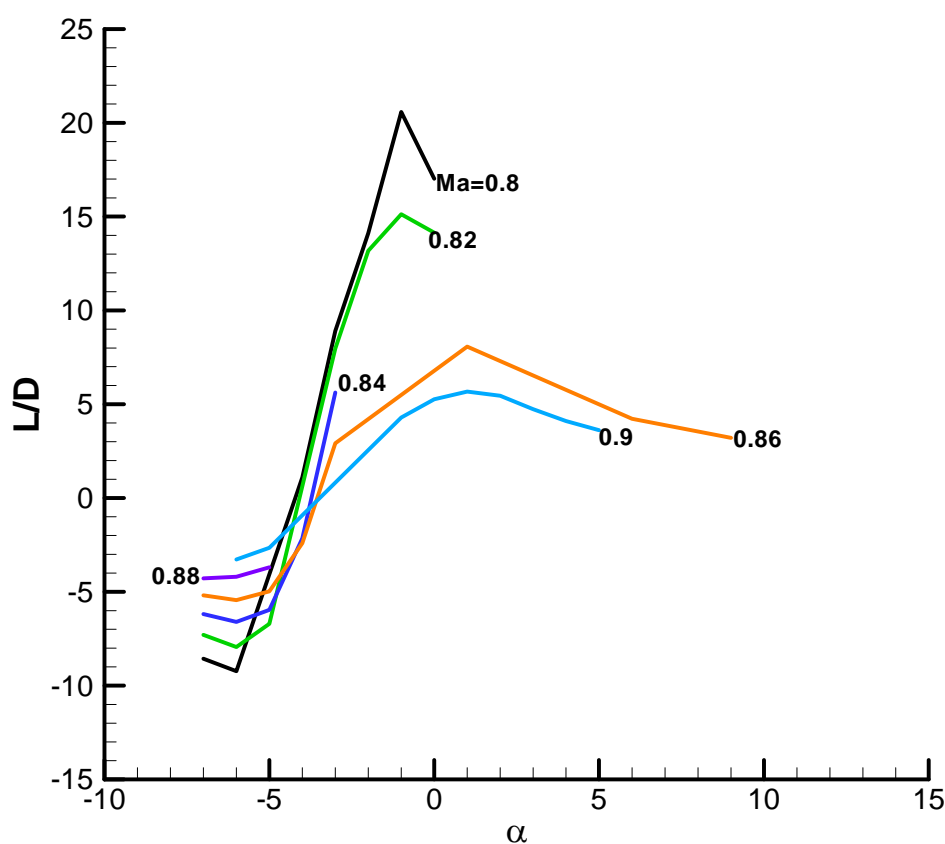


(b) $Ma=0.8 \sim 0.9$.

Fig. 13 Lift-to-drag ratio v.s. lift coefficient at different Mach numbers.

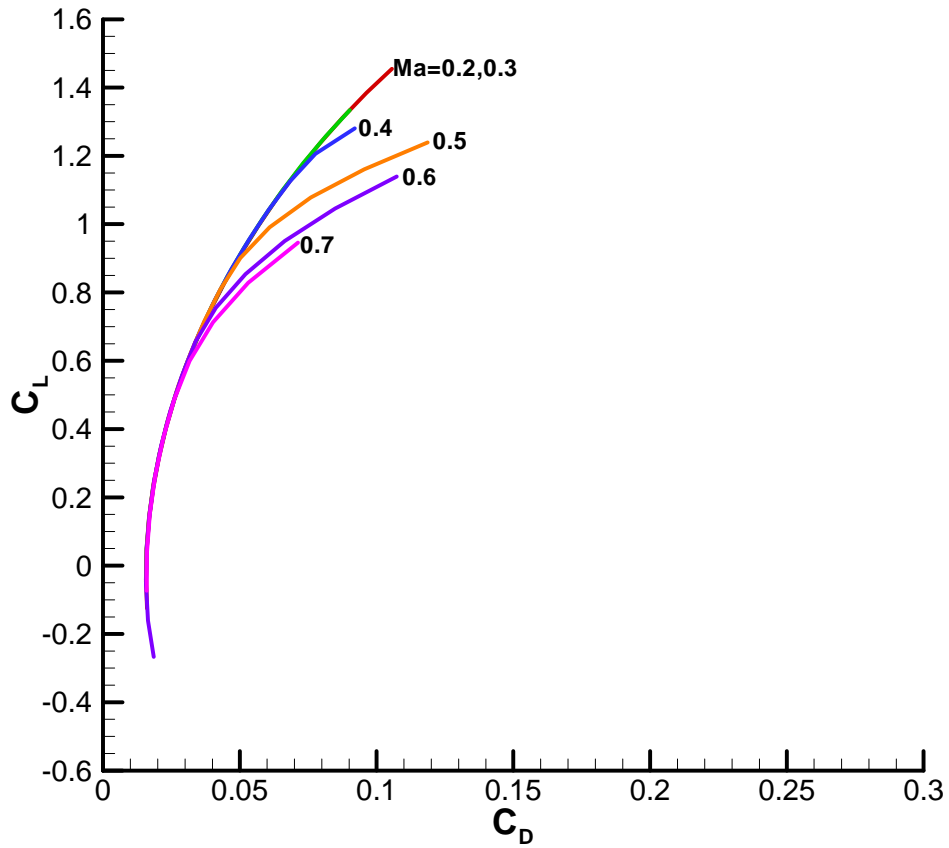


(a) $Ma=0.2 \sim 0.7$.

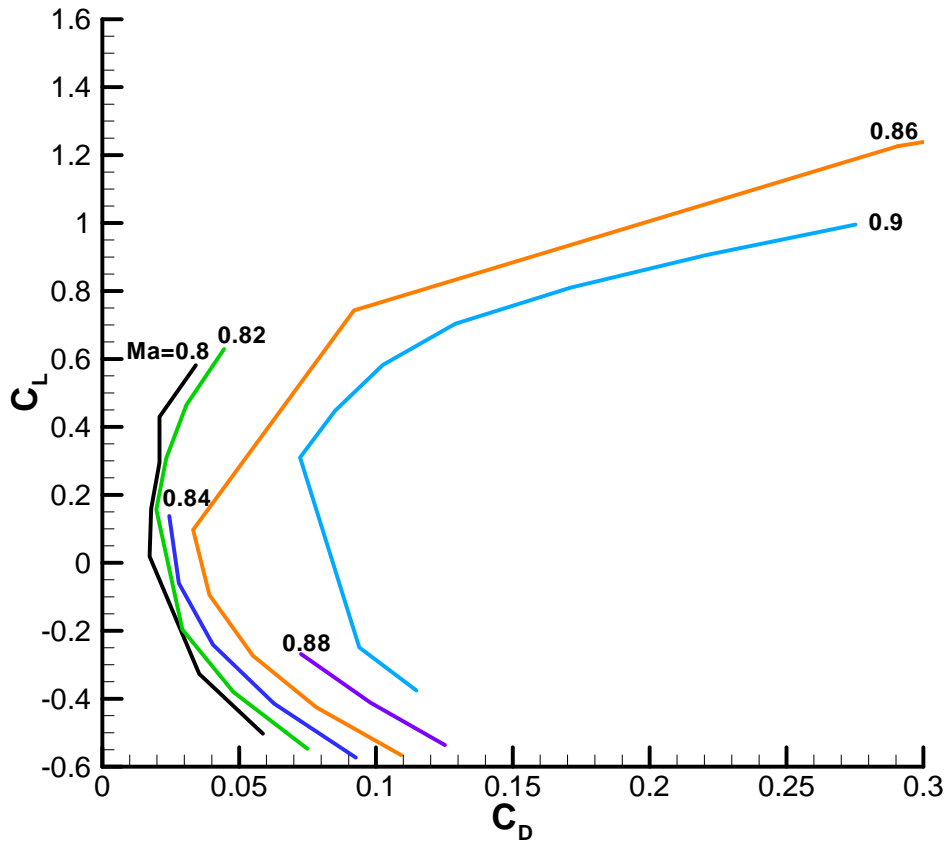


(b) $Ma=0.8 \sim 0.9$.

Fig. 14 Lift-to-drag ratio v.s. angle of attack in different Mach numbers.

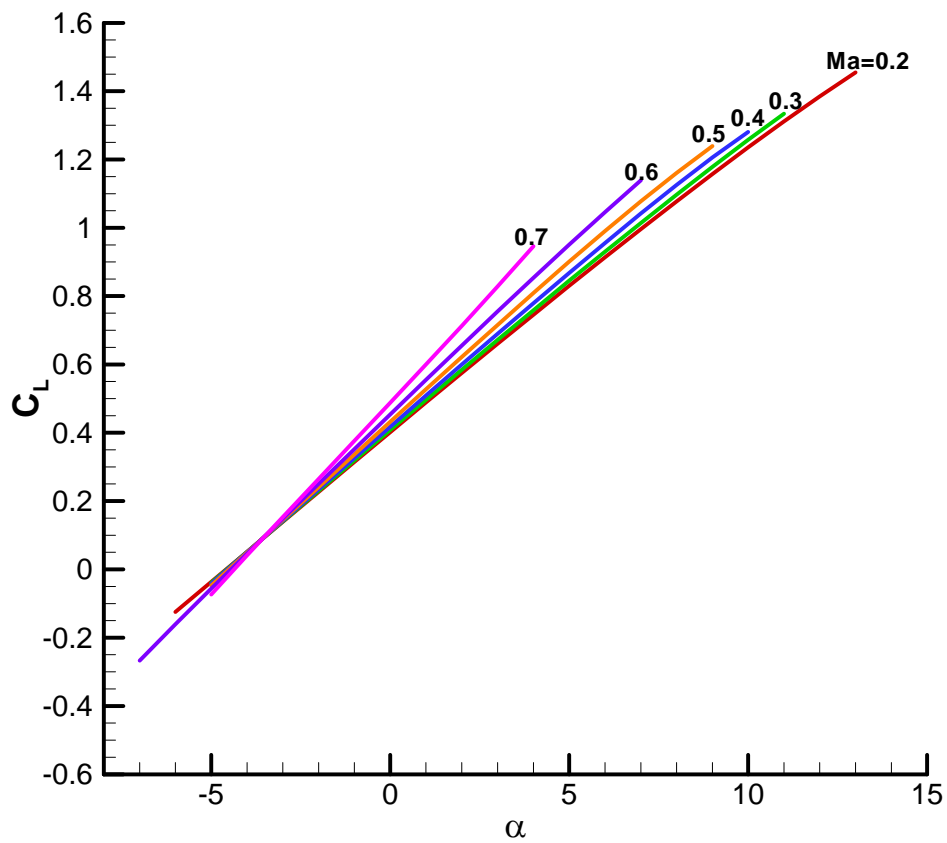


(a) $Ma=0.2 \sim 0.7$.

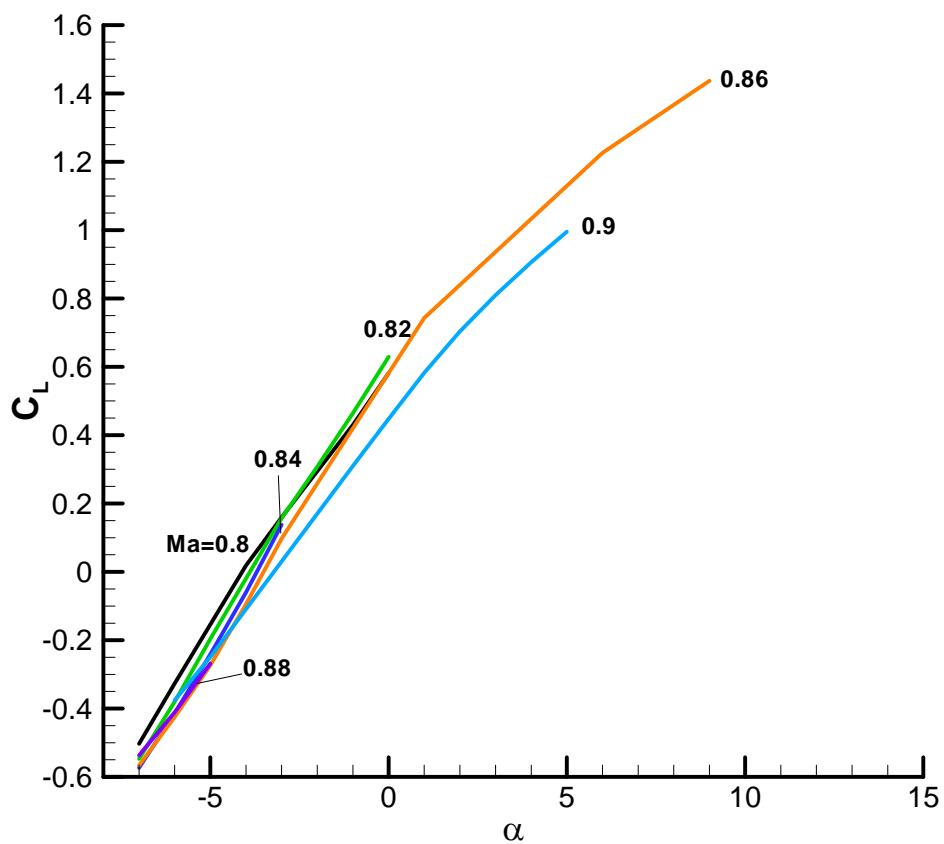


(b) $Ma=0.8 \sim 0.9$.

Fig. 15 Lift coefficient v.s. drag coefficient at different Mach numbers.

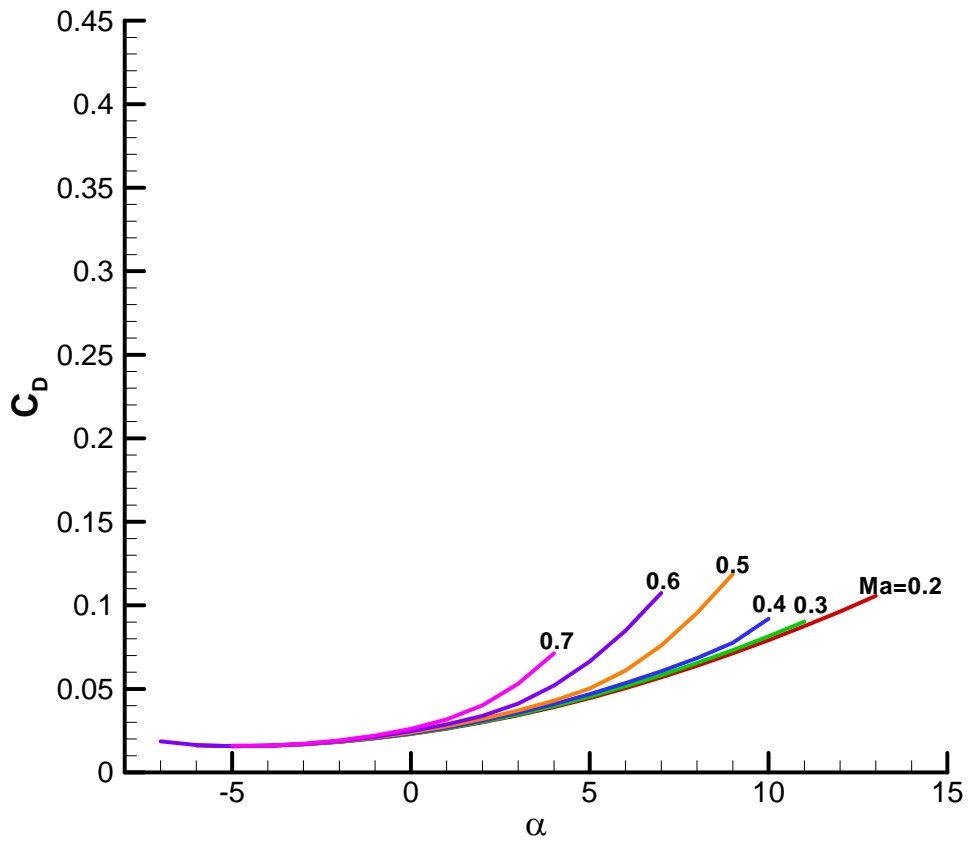


(a) $Ma=0.2 \sim 0.7$.

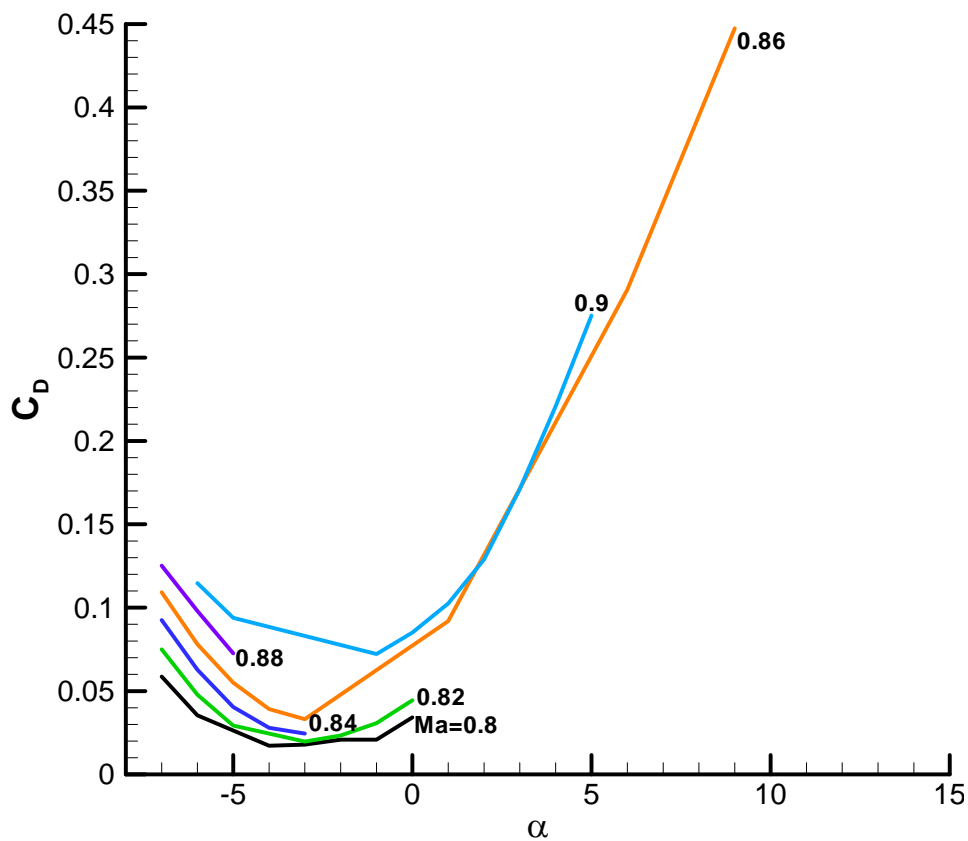


(b) $Ma=0.8 \sim 0.9$.

Fig. 16 Lift coefficient v.s. angle of attack at different Mach numbers.

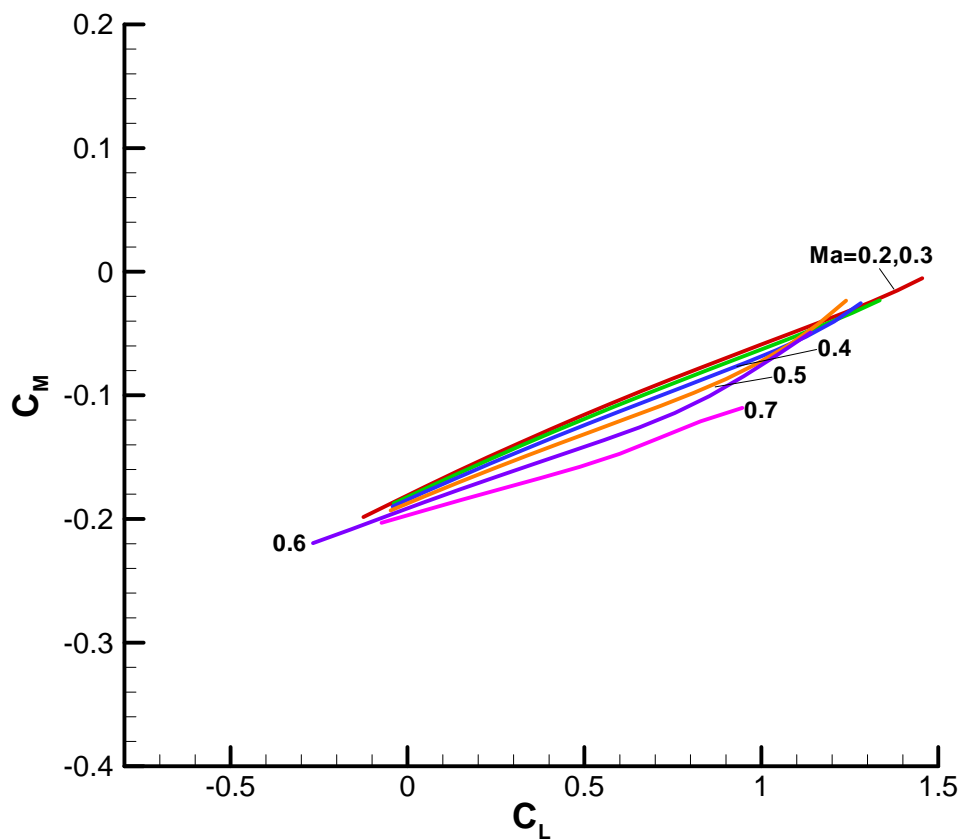


(a) $Ma=0.2 \sim 0.7$.

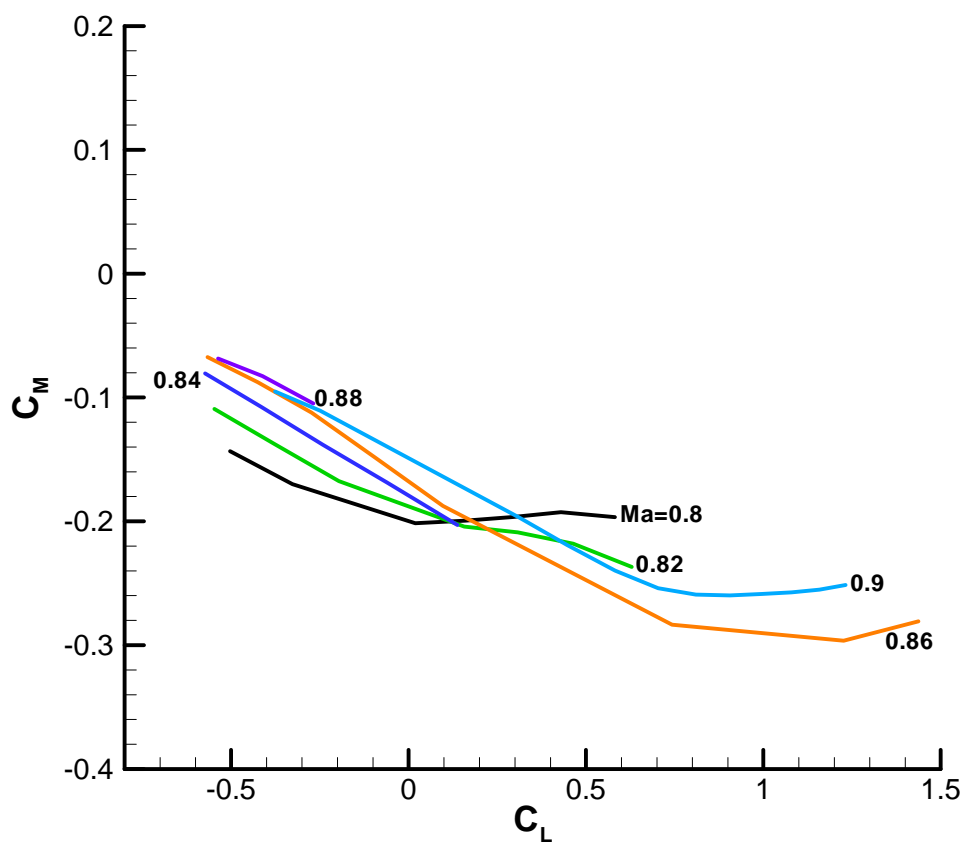


(b) $Ma=0.8 \sim 0.9$.

Fig. 17 Total drag coefficient v.s. angle of attack at different Mach numbers.

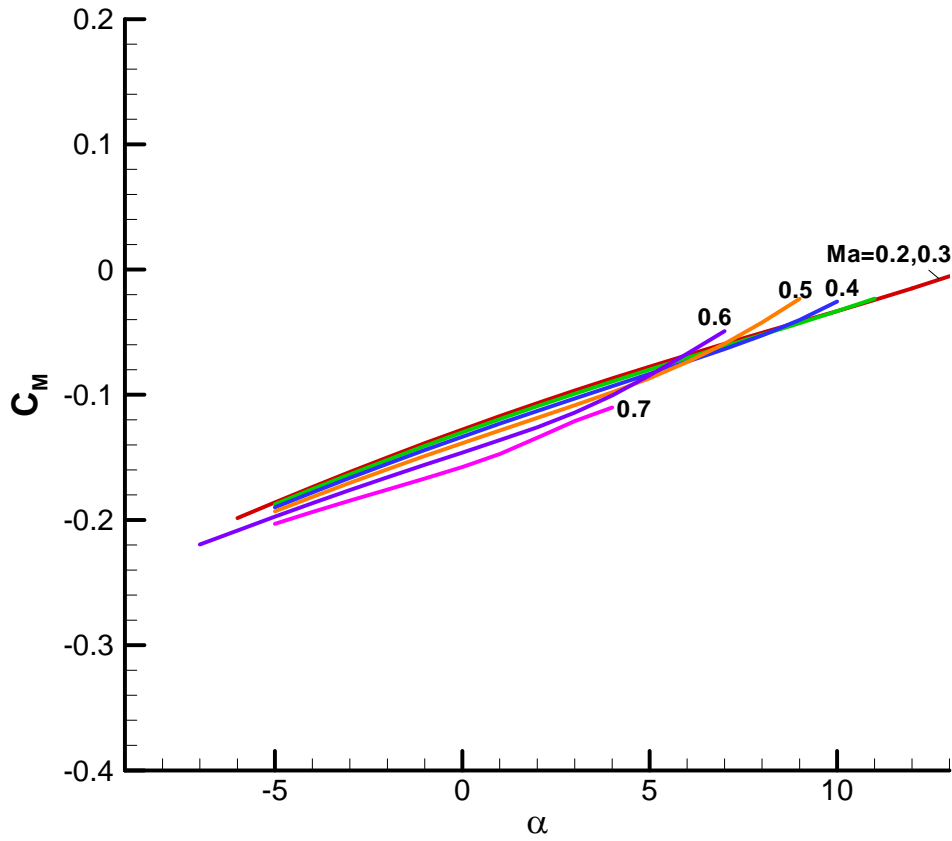


(a) $Ma=0.2 \sim 0.7$.

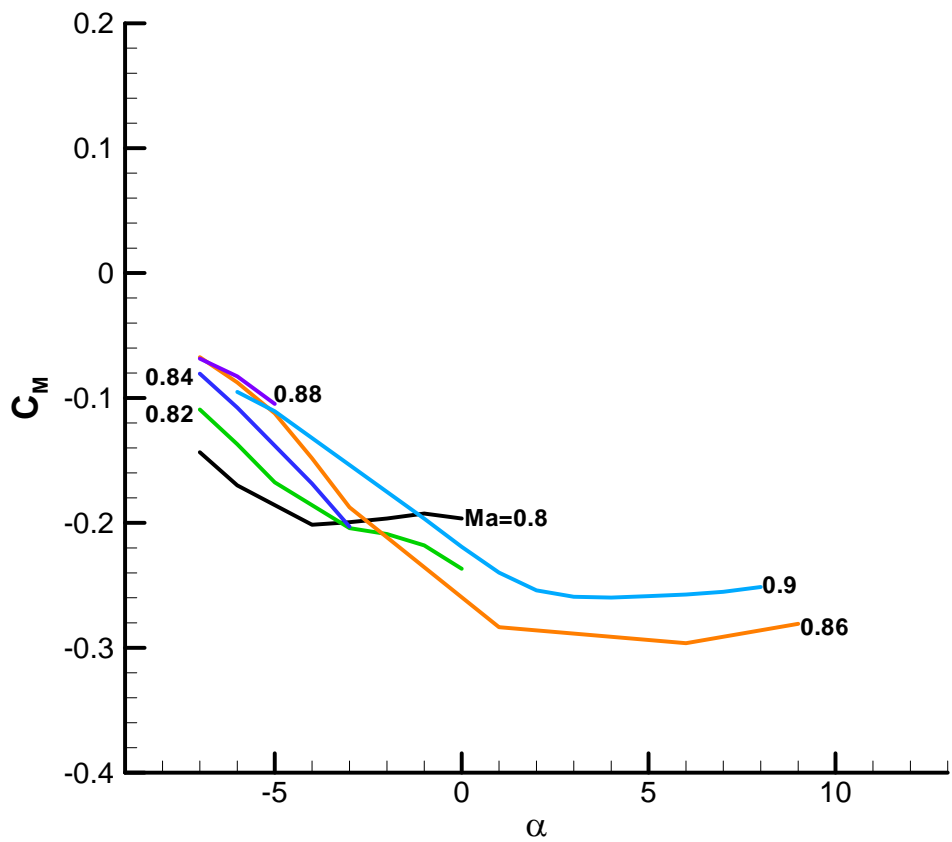


(b) $Ma=0.8 \sim 0.9$.

Fig. 18 Pitching moment coefficient v.s. lift coefficient at different Mach numbers.



(a) $Ma=0.2 \sim 0.7$.



(b) $Ma=0.8 \sim 0.9$.

Fig. 19 Pitching moment coefficient v.s. angle of attack at different Mach numbers.

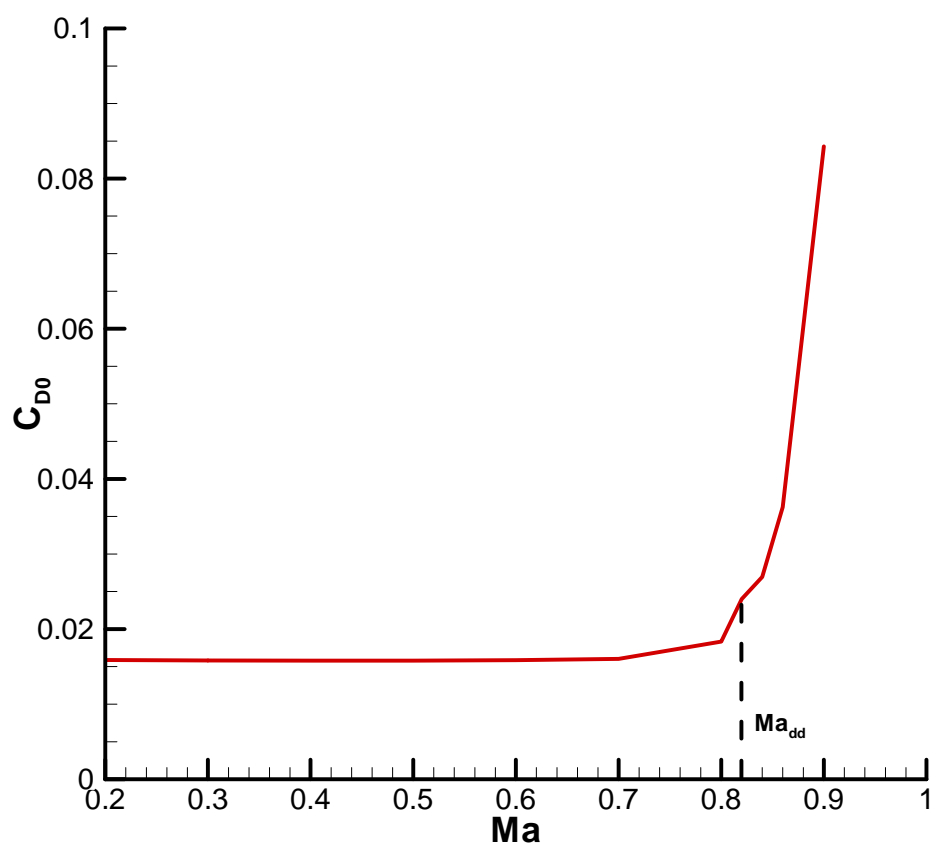


Fig. 20 Zero-lift drag coefficient v.s. Mach number .



IB 124-2010/3

**Evaluation of the BLWF Code –
A Tool for the Aerodynamic Analysis
of Transonic Transport Aircraft Configurations**

Ke-shi Zhang, Martin Hepperle

Copyright © 2010 – DLR

Deutsches Zentrum für Luft- und Raumfahrt e.V.
German Aerospace Center

Distribution List

Receiver	copies
Prof. Dr. Rossow	1
Dr. H. Geyr von Schweppenburg	1
Dr. Ke-Shi Zhang	1
Dr. M. Hepperle	2
Institutsbibliothek (C. Grant)	1
Deutsche Bibliothek in Frankfurt/Main	2
Niedersächsische Landesbibliothek Hannover	1
Techn. Informationsbibliothek Hannover	1
Zentralbibliothek BS	2
Reserve (C. Grant)	3
<hr/>	
total	15 copies